Journal Of Engineering And Technology Innovation (JETI)
Februari 2026 | Vol. 3 | No. 01
E-ISSN : 2828-0288
DOI: https://doi.org/10.66084/jeti.v3i01.598

Adaptive Fuzzy-PID Auto-Tuning for DC Motor Speed Control Under Varying Damping Coefficients

Halim Mudia*[1], Apriska Prameswari[2], Audy[3] , David Eka Putra[4], Firdaus[5]
[1,2,3,4,5] Jurusan Teknik Elektro - Politeliteknik Negeri Padang, Padang, Indonesia
e-mail: *[1]halim@pnp.ac.id , [2]apriska@pnp.ac.id , [3]audy@pnp.ac.id ,
[4]davidekaputra@pnp.ac.id , [5]mrdauz@pnp.ac.id

Abstract

DC motors are common in industry due to their simplicity, reliability, and ease of control. However, their speed regulation is sensitive to parameter changes and load disturbances. Variations in parameters like damping coefficients, caused by friction, temperature, and wear, can impair fixed-gain PID controllers. This paper introduces an adaptive fuzzy-PID auto-tuning (AFPAT) scheme to ensure robust speed control amid uncertainties and load disturbances. The controller uses a Sugeno fuzzy system to adjust PID gains online based on speed error (e) and derivative error (de). A second-order DC motor model assesses robustness by varying damping coefficients across five scenarios ($4.54 \leq a1 \leq 13.62$) and a 50 rpm load disturbance at 900 rpm setpoint. Performance measures include steady-state error, overshoot, settling time, and recovery time post-disturbance. Results show the controller achieves zero steady-state error and overshoot with settling times from 2.74 to 4.28 seconds and recovery times from 3.05 to 4.58 seconds. Compared to open-loop, with a steady-state error of 2963, the controller demonstrates robust speed regulation under parameter variations and disturbances.

Keyword : Adaptive Fuzzy-PID Controller, Auto-Tuning, DC Motor Speed Control System, Damping Coefficient and Load Variations.

INTRODUCTION

Direct current (DC) motors continue to play an essential role in industrial applications, including automation systems, robotics, and electric drives, owing to their high efficiency, fast dynamic response, and ease of speed control [1]. Nevertheless, the performance of DC motor speed control systems remains highly sensitive to parameter variations and external load disturbances encountered in real-world operating conditions [2]. Variations in motor parameters, particularly damping-related coefficients, arising from frictional changes, temperature effects, and mechanical wear, can significantly alter system dynamics and degrade control performance if not properly addressed [3]. These challenges necessitate advanced control strategies capable of maintaining performance under varying operating conditions.

Proportional–integral–derivative (PID) controllers remain widely employed in industrial motor control systems due to their simple structure and ease of implementation [4]. However, conventional PID controllers are typically tuned using nominal motor models and fixed operating conditions [5]. When system parameters vary or sudden load disturbances occur, fixed-gain PID controllers often exhibit increased steady-state error (E_{ss}), oscillatory responses, or slow recovery, making them unsuitable for systems operating in dynamic environments [5], [6]. Several studies have attempted to improve PID performance through optimisation-based tuning methods [7], [8]. However, these approaches typically require offline tuning and cannot adapt to real-time parameter changes.

To address these limitations, intelligent control approaches, including fuzzy logic control and fuzzy-PID schemes, have been extensively investigated in recent years. Fuzzy logic controllers provide an effective means of handling nonlinearities and uncertainties without requiring precise mathematical models [9]. Recent studies have shown that fuzzy-PID controllers can enhance transient performance and reduce steady-state error (E_{ss}) in DC motor speed control applications [10], [11]. For instance, Bhayo et al. [10] proposed an adaptive neuro-fuzzy inference system (ANFIS) controller that achieved significant improvements in settling time (T_s) and steady-state error (E_{ss}) compared with a conventional PID controller. Similarly, Al-Dabbagh and Shneen [11] demonstrated that neuro-fuzzy controllers outperform traditional PID controllers in disturbance rejection and transient response. However, most of these studies assume fixed motor parameters or rely on offline system identification, limiting their adaptability to real-time changes in motor dynamics.

More recent research has focused on adaptive control and online identification techniques to address parameter uncertainty and load disturbances [12], [13], [14]. Kristiyono and Wiyono [12] proposed a fuzzy-PID auto-tuning controller for BLDC motors with online adaptation. At the same time, Rospawan et al [13] developed an adaptive nonlinear PID using polynomial fuzzy LSTM neural networks for system identification. Although these approaches improve robustness, they typically focus on either adaptive control or system identification, with limited systematic evaluation across wide ranges of parameter variations. Furthermore, most existing studies evaluate controller performance under nominal or narrowly ranged operating conditions, without comprehensive testing across systematic parameter variations that represent motor ageing, temperature effects, and friction changes, combined with external load disturbances.

Despite these advancements, a critical gap remains: existing approaches do not provide a comprehensive evaluation of fuzzy-PID performance across systematic, wide-ranging variations in damping coefficients that reflect realistic motor operating conditions. This gap is significant because real-world DC motors in industrial applications experience simultaneous parameter variations (due to frictional changes, temperature fluctuations, and mechanical wear) and external disturbances, necessitating controllers that maintain robust performance across diverse operating conditions. While papers such as [10] and [12] demonstrate the effectiveness of fuzzy-PID, their evaluations typically cover only one or two operating conditions and lack a systematic analysis across multiple parameter scenarios.

Motivated by this research gap, this paper proposes an adaptive fuzzy-PID auto-tuning control scheme for DC motor speed control that maintains performance despite wide variations in the damping coefficient. A Sugeno-type fuzzy inference system automatically adjusts the PID controller gains based on the speed error (e) and the derivative error (de), thereby providing computational efficiency suitable for real-time implementation. The DC motor is modelled as a second-order system with a variable damping parameter that accounts for motor uncertainty arising from frictional changes, temperature effects, and mechanical wear. The key contribution of this work is a systematic and comprehensive evaluation of adaptive fuzzy-PID performance across five damping coefficient scenarios spanning a 300% range ($4.54 \leq a1 \leq 13.62$), together with sudden-load disturbance testing. This evaluation demonstrates that the controller maintains zero steady-state error (E_{ss}) and zero per cent maximum overshoot (M_p), and achieves rapid disturbance recovery across all tested conditions, providing quantitative evidence of robustness superior to conventional fixed-gain approaches.

RESEARCH METHODS

A. DC motor mathematical model

The DC motor model is based on the standard armature-controlled representation from control texts like Ogata's Modern Control Engineering, with coupled differential equations for electrical and mechanical parts. The armature circuit follows Kirchhoff's voltage law [15]

$$V_a(t) = R_a i_a(t) + L_a \frac{di_a(t)}{dt} + K_e \omega(t) \quad (1)$$

While Newton's second law governs rotor dynamics:

$$J\frac{d\omega(t)}{dt} = K_T i_a(t) - B\omega(t) - T_L(t) \quad (2)$$

Where $V_a(t)$ represents the armature voltage, R_a and L_a are the armature resistance and inductance respectively, $i_a(t)$ indicates the armature current, K_e is the back-EMF constant, $\omega(t)$ denotes the angular speed, J stands for the rotor inertia, K_T is the torque constant, B signifies the viscous damping coefficient, and $T_L(t)$ is the load torque. Assuming operation in SI units, where $K_T = K_e$, and noting that the electrical time constant $\tau_e = L_a/R_a$ is typically much smaller than the mechanical time constant τ_m = J/B, the inductance term can be neglected ($La \approx 0$), yielding a reduced second-order transfer function between speed and voltage [16]:

$$G_P(s) = \frac{\omega(s)}{V_a(s)} = \frac{K_m}{s^2 + a_1 s + a_0} \quad (3)$$

Km is the motor gain, a_1 the effective damping coefficient, and a_0 relates to the system's squared natural frequency. This second-order model, common in recent DC motor control work, captures main dynamics while being simple enough for controller design and parameter identification.

For the specific motor, K_m, a_0, and a_1 are determined experimentally via system identification rather than from datasheets. Donjaroennon et al. used MATLAB's System Identification Toolbox to collect speed data at 800-1000 rpm and then converted the closed-loop model into an open-loop plant. The resulting second-order transfer function is [17]:

$$G_P(s) = \frac{\omega(s)}{V_a(s)} = \frac{71.43}{s^2 + 9.08s + 16.64} \quad (4)$$

Where $\omega(s)$ denotes the Laplace transform of the motor angular speed $\omega(t)$, $V_a(s)$ is the Laplace transform of the applied armature voltage $V_a(t)$, 71.43 represents the motor gain K_m, 9.08 is the identified damping-related coefficient a_1, and 16.64 corresponds to the term a_0 associated with the system's squared natural frequency.

B. Parameter variations for DC motor

To analyse robustness to parameter variations, the damping coefficient a_1 is varied to represent different friction conditions in the DC motor. These variations can be interpreted as arising from friction, thermal effects, and mechanical wear of the rotor–shaft assembly [18]. The values of a_1 for each scenario are summarised in Table I.

Each scenario corresponds to a different instance of the plant transfer function for the DC motor:

Table 1 Damping-related coefficient scenarios

Scenario	a_1	Qualitative damping condition
1	4.54	Under-damped
2	6.81	Lightly damped (under-damped with moderate damping)
3	9.08	Nominal damping (identified model)
4	11.3	Over-damped
5	13.62	Heavily damped (over-damped with very high damping.)

$$G_{P,i}(s) = \frac{71.43}{s^2 + a_{1,i} s + 16.64} \quad i \in \{1,2,3,4,5\} \quad (5)$$

When a_{1i} is selected according to Table I, the range of a_1 values spans a 300% variation relative to the lowest-damping case, providing a wide test envelope for evaluating controller robustness under substantial parameter uncertainty. Such systematic variation of a single dominant parameter is common in recent DC motor modelling and robustness studies, enabling a clear assessment of how changes in effective damping affect speed response and control performance [19].

C. Problem formulation and disturbance scenario

The control objective of the DC motor drive is to regulate the rotor speed to a constant reference speed (setpoint), $\omega_{ref}(t)$ = 900 rpm, under nominal conditions and across parameter variations. The control error is defined as:

$$e(t) = \omega_{ref}(t) - \omega(t) \quad (6)$$

Where ω(t) denotes the measured speed (output), the closed-loop response must satisfy the following specifications across all considered damping-coefficient scenarios: zero steady-state error (E_{ss}) to the step reference speed (setpoint), maximum overshoot (M_p)≤ 5%, and settling time (T_s)≤ 5 s using the 2% criterion. In addition, the system must be robust to load disturbances, so that when a step-like load causing an equivalent 50 rpm speed drop is applied at t = 10 s, the speed recovers to within 2% of the reference speed (setpoint), in less than 5 s.

In this work, the load disturbance is modelled as an external torque applied to the motor shaft that increases instantaneously at t = 10 s, causing an approximate 50 rpm decrease in the steady-state speed in the absence of any control action. The designed controller must therefore ensure accurate reference speed (setpoint) tracking and effective rejection of this disturbance for all specified damping-coefficient variations.

D. Adaptive Fuzzy-Pid Auto-Tuning (AFPAT) System

1) System overview

Picture 1 shows the overall structure of the proposed adaptive fuzzy-PID auto-tuning system for DC motor speed control. The reference speed (setpoint) is compared with the measured speed (output) to generate the control error *e(t)*. Together with its delta error *(de)*, this error is processed by the fuzzy-PID auto-tuning block to produce the control signal *u(t)* applied to the DC motor drive. Within the fuzzy-PID block, a fuzzy inference mechanism adapts the proportional (*Kp*), integral (*Ki*), and derivative (*Kd*) gains online based on the current operating condition, enabling the closed-loop system to maintain the desired transient and steady-state performance despite parameter variations and load disturbances.

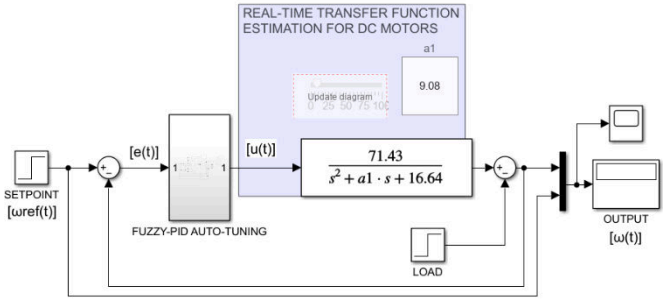

Picture 1 Block diagram of the proposed adaptive fuzzy-PID auto-tuning control system for DC motor speed regulation

2) Fuzzy-PID Auto-Tuning Design

The proposed auto-tuning mechanism is implemented using a Sugeno-type fuzzy inference system (FIS) that adjusts the PID gains online in response to the dynamics of the speed

error (*e*). In Picture 2, the FIS has two input variables, the speed error (*e*) and the delta error (*de*), and three output variables corresponding to the proportional (*Kp*), integral (*Ki*), and derivative (*Kd*) gains.

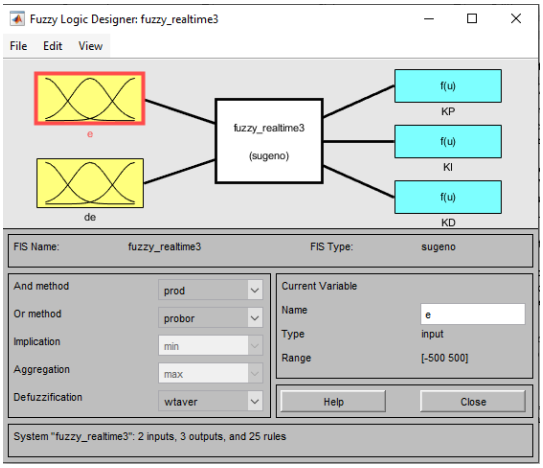

Picture 2 Design of sugeno-type fuzzy inference system (FIS)

In Picture 3-5, we can predict the values of *e, de, Kp, Ki*, and *Kd* based on our experience with the DC motor.

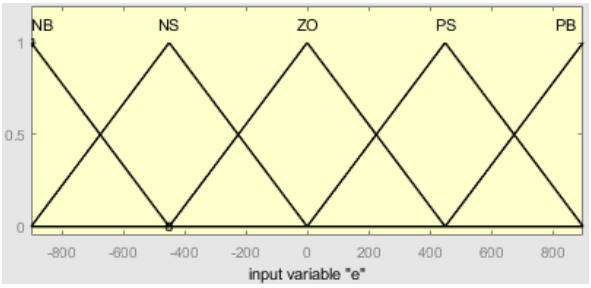

Picture 3 Membership functions of error (*e*) with range -900 to 900

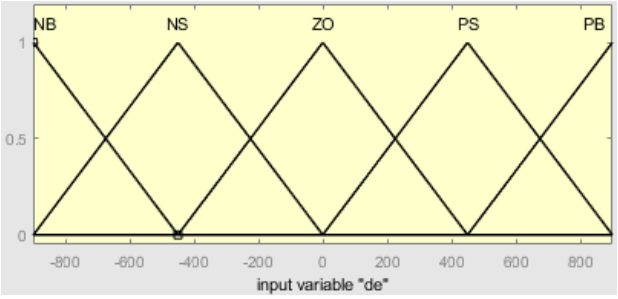

Picture 4 Membership functions of derivative error (*de*) with range -900 to 900

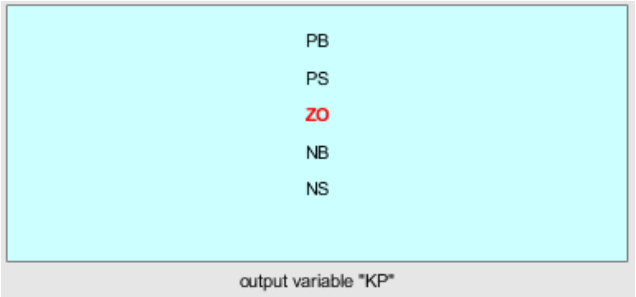

Picture 5 Membership functions of Kp

The singleton membership functions for *Ki* and *Kd* are the same as in Figure 5, but with a different range of values, obtained from experience with the DC motor's transfer function. In this design, the proportional gain (*Kp)* is defined in the range [0 to 0.38], the integral gain (*Ki)* in the range [0 to 0.7], and the derivative gain (*Kd)* in the range [0 to 0.042].

Since a Sugeno-type controller with singleton outputs is used, each linguistic term corresponds directly to a constant gain value rather than a triangular Mamdani membership function. For all three gains, the five linguistic levels {NS, ZO, PS, PB} are uniformly distributed over the positive range, with NS = 0 and the remaining singletons spaced at equal intervals up to the corresponding maximum value. Specifically, for *Kp* is NS = 0, ZO = 0.127, PS = 0.253, and PB = 0.38; for *Ki* is NS = 0, ZO = 0.233, PS = 0.467, and PB = 0.70; and for Kd is NS = 0, ZO = 0.014, PS = 0.028, and PB = 0.042. These uniformly spaced singleton values provide a simple yet effective mapping from the fuzzy rule base to the adaptive PID gains within the Sugeno inference framework, as applied to the rule base in the Table of Macvicar Whelan [20].

Table 2 Macvicar whelan rule base

Kp, Ki, Kd		de				
		NB	*NS*	*ZO*	*PS*	*PB*
e	NB	PB	PB	PB	PS	ZO
	NS	PB	PB	PS	ZO	NS
	ZO	PB	PS	ZO	NS	NB
	PS	PS	ZO	NS	NB	NB
	PB	ZO	NS	NB	NB	NB

The 25 fuzzy rules define how the PID gains are adjusted based on the current speed error (*e*) and derivative error (*de*), with both inputs using five linguistic terms: NB (Negative Big), NS (Negative Small), ZO (Zero), PS (Positive Small), and PB (Positive Big). The same linguistic output selected by each rule is applied to all three gains, *Kp*, *Ki*, and *Kd*. However, their actual numerical values differ according to their respective output membership functions.

More specifically, when both the error (*e*) and derivative error (*de*) are strongly negative (NB or NS), the rules assign high positive gains (PB or PS), prompting the controller to respond aggressively to reduce the error (*e*) quickly. As the error (*e*) and derivative error (*de*) approach zero (ZO), the rules gradually reduce the gains from PB/PS to ZO, providing smoother control action around the operating point and preventing excessive maximum overshoot (M_p). When the error (*e*) becomes positive (PS or PB), and the derivative error (*de*) indicates that the speed is increasing towards or beyond the reference speed (setpoint), the rules switch the gains to smaller or even negative linguistic levels (NS, NB), effectively weakening or reversing the control effort to avoid maximum overshoot (M_p) and bring the speed back towards the reference speed (setpoint).

Overall, the rule base is symmetric: large-magnitude errors (NB or PB) combined with derivative error (*de*) of the same sign produce decisive corrective actions in the opposite direction, while combinations where error (*e*) and derivative error (*de*) have opposite signs yield more moderate gains. This structure ensures that the adaptive fuzzy-PID auto-tuning controller responds strongly when the motor speed deviates from the reference speed (setpoint), thereby improving both transient response and steady-state accuracy.

RESULTS AND DISCUSSION

A. Step-response comparison at nominal operating condition

This subsection investigates the behaviour of the DC motor at the nominal damping-related coefficient $a1$ = 9.08, corresponding to the identified plant model. The experiment considers a 900 rpm reference speed (setpoint) and a 50 rpm load disturbance applied at t = 10 s. Picture 6-7 shows the speed responses of the open-loop system and the proposed adaptive fuzzy-PID auto-tuning controller under these conditions.

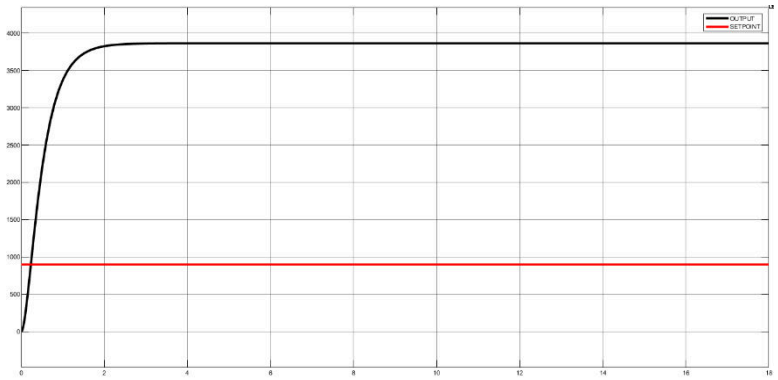

Picture 6 Speed response output of the open-loop system with a_1=9.0

In the open-loop configuration, the motor is driven by a fixed input voltage selected during the identification procedure. The measured speed (output) rises rapidly but converges to a steady-state speed of 3863 rpm, rather than the reference speed (setpoint) of 900 rpm. This corresponds to a large steady-state error (E_{ss}) of 2963 rpm, which is identical across all damping scenarios because the final value is determined by the plant gain rather than the damping coefficient. The maximum overshoot (M_p) for the nominal case is 0%, and the 2% settling time (T_s) is approximately 1.73 s. Although the open-loop response is fast, it is entirely inaccurate relative to the reference speed (setpoint).

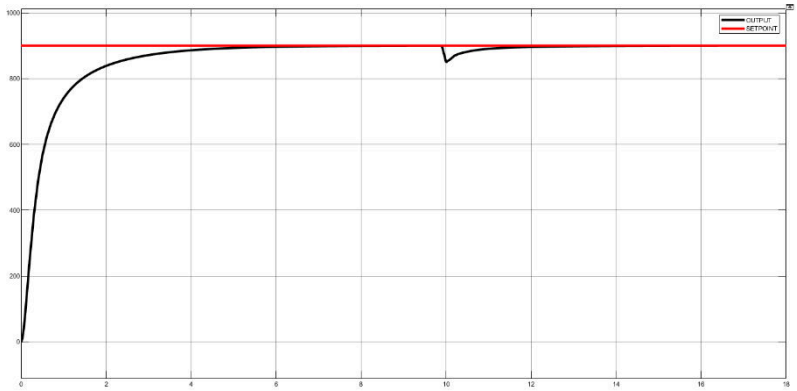

Picture 7 Speed and load disturbance responses of a system of an adaptive fuzzy-PID auto-tuning controller with a_1 =9.08

The adaptive fuzzy-PID auto-tuning controller is then activated while the nominal plant is maintained. As shown in Figure 7, the closed-loop speed response closely follows the 900 rpm reference speed (setpoint), with a smooth, monotonic rise. The steady-state error (E_{ss}) is 0 rpm, and the maximum overshoot (M_p) is 0 %, indicating that the fuzzy inference mechanism delivers a well-damped response at the nominal operating point. The settling time (T_s) increases to 3.64 s, exceeding the open-loop value but remaining well below the design specification of 5 s.

At t = 10 s, a step load disturbance equivalent to a 50-rpm speed drop is applied to simulate a sudden decrease in mechanical torque. In the open-loop case, the motor speed settles

at a new value and does not return to the original steady state because there is no feedback signal to counteract the disturbance. Under the adaptive fuzzy-PID auto-tuning controller, the disturbance causes a temporary speed dip, but the controller automatically adjusts its gains and drives the speed back to the reference speed (setpoint), with the response reentering the 2% band around 900 rpm in approximately 3.96 s. The comparison in Figures 6 and 7, therefore, highlights two critical improvements at the nominal condition: the elimination of significant open-loop steady-state error (E_{ss}) and the introduction of effective disturbance rejection.

B. Quantitative comparison with open-loop operation

To complement the qualitative analysis of the response plots, the time-domain metrics from the simulations are summarised in Table III. For each damping scenario, the table lists the steady-state error (E_{ss}), maximum overshoot (M_p), settling time (T_s), and disturbance-recovery time (T_{Rec}) for both open-loop and closed-loop (adaptive fuzzy-PID auto-tuning (AFPAT)) configurations.

Table 3 Time-domain performance across damping-coefficient scenarios

$a1$	Mode	*Ess* (rpm)	*Mp* (%)	*Ts* 2% (s)	(T_{Rec}) (s)
4.54	Open-loop	2963	12.1304	0.6210	-
6.81	Open-loop	2963	0.8652	0.9936	-
9.08	Open-loop	2963	0	1.7302	-
11.35	Open-loop	2963	0	2.3750	-
13.62	Open-loop	2963	0	2.9673	-
4.54	AFPAT	0	0	4.2765	4.5790
6.81	AFPAT	0	0	3.9883	4.2972
9.08	AFPAT	0	0	3.6441	3.9598
11.35	AFPAT	0	0	3.2029	3.5346
13.62	AFPAT	0	0	2.7359	3.0495

This quantitative comparison shows that the open-loop system, while sometimes faster in raw settling time, is fundamentally unsuitable for precision speed regulation because it exhibits a large, parameter-independent steady-state error (E_{ss}), cannot reject load disturbances, and may produce significant overshoot in lightly damped motors. The adaptive fuzzy-PID auto-tuning controller, by contrast, trades a modest increase in settling time (T_s) for substantial gains in accuracy, damping, and robustness to both parameter variations and disturbances.

CONCLUSION

This paper presents an adaptive fuzzy-PID auto-tuning (AFPAT) scheme for DC motor speed control under systematic variations in the damping-related coefficient and step-like load disturbances. The proposed Sugeno-type fuzzy inference system adjusts the PID gains online based on the speed error (e) and derivative error (de), enabling robust performance without retuning over a 300% variation in the damping parameter. Simulation results show that, across all

considered damping scenarios, the controller achieves a steady-state error (E_{ss}) of 0 rpm and a maximum overshoot (M_p) is 0 %, while maintaining settling times below 5 s and disturbance-recovery times below 5 s for a 50 rpm load-induced speed drop. Compared with open-loop operation, which exhibits a fixed steady-state error (E_{ss}) of 2963 rpm and no disturbance-rejection capability, the adaptive fuzzy-PID controller provides accurate tracking and effective disturbance rejection over the entire operating range. These findings indicate that the proposed approach is a promising candidate for DC motor drive applications subject to parameter uncertainties and varying mechanical loads.

SUGGESTION

From a practical standpoint, the findings suggest that the proposed controller can be deployed in industrial DC motor drives where operating conditions vary due to ageing or changing loads, with minimal manual retuning. The fuzzy PID structure remains relatively interpretable and straightforward, relying on a compact rule base and a small number of singleton gains, thereby facilitating implementation on low-cost microcontrollers or digital signal processors commonly used in motor drives. Future work could extend this approach to include additional sources of uncertainty, such as variations in motor gain or load inertia, and to validate the controller on hardware-in-the-loop or experimental test beds to complement the simulation-based evidence presented here.

BIBLIOGRAPHY

[1] I. Husain, B. Ozpineci, M. S. Islam, E. Gurpinar, G.-J. Su, W. Yu, S. Chowdhury, L. Xue, D. Rahman, and R. Sahu, "Electric Drive Technology Trends, Challenges, and Opportunities for Future Electric Vehicles," *Proceedings of the IEEE*, vol. 109, no. 6, pp. 1115–1135, 2021, doi: 10.1109/JPROC.2020.3046112.

[2] M. Jabari, S. Ekinci, D. Izci, M. Bajaj, and I. Zaitsev, "Efficient DC motor speed control using a novel multi-stage FOPD(1 + PI) controller optimized by the Pelican optimization algorithm," *Scientific Reports*, vol. 14, no. 22442, 2024, doi: 10.1038/s41598-024-73409-5.

[3] P. Wang, J. Zhao, and K. Liu, "Parameter-Adaptation-Based Virtual DC Motor Control Method for Energy Storage Converter," *IEEE Access*, vol. 9, pp. 94375–94386, 2021, doi: 10.1109/ACCESS.2021.3091699.

[4] A. Turan, "Improved PID Control Design for Electric Power Steering DC Motor," *IEEE Access*, vol. 13, pp. 183–196, 2025, doi: 10.1109/ACCESS.2024.3524303.

[5] C. Naveen, S. S. Chauhan, C. Paramasivam, and V. P. Meena, "FPGA IP Core for DC Motor Control With Adaptive Neural Network PID Tuning, and High-Resolution Encoder Interface," *IEEE Access*, vol. 12, pp. 151158–151171, 2024, doi: 10.1109/ACCESS.2024.3491995.

[6] B. Hekimoğlu, "Optimal Tuning of Fractional Order PID Controller for DC Motor Speed Control via Chaotic Atom Search Optimization Algorithm," *IEEE Access*, vol. 7, pp. 38100–38114, 2019, doi: 10.1109/ACCESS.2019.2905961.

[7] A. Singh, S. Yadav, N. Tiwari, D. K. Nishad, and S. Khalid, "Optimized PID controller and model order reduction of reheated turbine for load frequency control using teaching learning-based optimization," *Scientific Reports*, vol. 15, Art. no. 3759, 2025, doi: 10.1038/s41598-025-87866-z.

[8] H. Maghfiroh, M. Nizam, M. Anwar, and A. Ma'arif, "Improved LQR Control Using PSO Optimization and Kalman Filter Estimator," *IEEE Access*, vol. 10, pp. 15353–15367, 2022, doi: 10.1109/ACCESS.2022.3149815.

[9] D. Mohanraj, R. Aruldavid, R. Verma, K. Sathiyasekar, A. B. Barnawi, and B. Chokkalingam, "A Review of BLDC Motor: State of Art, Advanced Control Techniques, and

Applications," *IEEE Access*, vol. 10, pp. 54833–54869, 2022, doi: 10.1109/ACCESS.2022.3175011.

[10] M. A. Bhayo, J. A. Laghari, M. Aljaidi, M. A. Koondhar, R. A. El-Sehiemy, A. F. Alkoradees, and Z. M. Alaas, "High precision experimentally validated adaptive neuro fuzzy inference system controller for DC motor drive system," *Scientific Reports*, vol. 15, Art. no. 14445, 2025, doi: 10.1038/s41598-025-97549-4.

[11] Z. A. Al-Dabbagh and S. W. Shneen, "Neuro-Fuzzy Controller for a Non-Linear Power Electronic DC–DC Boost Converters," *Journal of Robotics and Control (JRC)*, vol. 5, no. 5, pp. 1479–1494, 2024, doi: 10.18196/jrc.v5i5.22690.

[12] R. Kristiyono and Wiyono, "Autotuning Fuzzy PID Controller for Speed Control of BLDC Motor," *Journal of Robotics and Control (JRC)*, vol. 2, no. 5, pp. 400–407, Sept. 2021, doi: 10.18196/jrc.v2i5.25114.

[13] A. Rospawan, C. L. Angelina, I. A. Setiawan, Z. Saputra, Ocrisrendi, A. Febriansyah, I. Dwisaputra, and R. Napitupulu, "Adaptive Nonlinear PID Control of DC Motor Position Using a Polynomial Fuzzy Long Short-Term Memory Neural Network," *International Journal of Automotive and Mechanical Engineering*, vol. 22, no. 3, pp. 12821–12836, 2025, doi: 10.15282/ijame.22.3.2025.20.0977.

[14] M. Liu, P. Shi, L. Zhang, and X. Zhao, "Fault-Tolerant Control for Nonlinear Markovian Jump Systems via Proportional and Derivative Sliding Mode Observer Technique," *IEEE Transactions on Circuits and Systems I: Regular Papers*, vol. 58, no. 11, pp. 2755–2764, Nov. 2011, doi: 10.1109/TCSI.2011.2157734.

[15] K. Ogata, *Modern Control Engineering*, 5th ed. Upper Saddle River, NJ, USA: Prentice Hall, 2010.

[16] N. N. A. Rahman and N. M. Yahya, "A mathematical model of a brushed DC motor system," *Data Analytics and Applied Mathematics (DAAM)*, vol. 2, no. 2, pp. 060–068, 2022, doi: 10.15282/daam.v2i2.6830.

[17] N. Donjaroennon, S. Nuchkum, and U. Leeton, "Mathematical model construction of DC motor by closed-loop system identification technique using MATLAB/Simulink," in *Proceedings of the 2021 9th International Electrical Engineering Congress (iEECON)*, Pattaya, Thailand, Mar. 10–12, 2021, doi: 10.1109/iEECON51072.2021.9440305.

[18] Nguyen, T. K., S. M. Vlasov, A. A. Margun, and A. S. Kirsanova, "Identification of DC Motor Parameters Using Method of Dynamic Regressor Extension and Mixing," in *Proc. 2021 29th Mediterranean Conference on Control and Automation (MED)*, Puglia, Italy, 22–25 June 2021, doi: 10.1109/MED51440.2021.9480165.

[19] M. J. Husseïn, O. T. Khazraji, and A. M. Almawla, "Simulation and experimental evaluation of DC motor control strategies using MATLAB and Arduino Mega," *J. Eur. Syst. Autom.*, vol. 58, no. 1, pp. 55–64, 2025, doi: 10.18280/jesa.580107

[20] A. Dhyani, M. K. Panda, and B. Jha, "Design of an evolving fuzzy-PID controller for optimal trajectory control of a 7-DOF redundant manipulator with prioritized sub-tasks," Expert Systems with Applications, vol. 162, Art. no. 113021, Dec. 2020, doi: 10.1016/j.eswa.2019.113021.